Proceedings of the 6th ITB International Graduate School Conference
Multidisciplinary Collaboration for Sustainable Energy: Science, Technology, Policy, and Society

Process Optimization of Carbon Capture and Storage in Coal Fired Power Plant with Heat Integration

Veri Hendrayawan[1,2], Anggit Raksajati[2] & Sanggono Adisasmito[2]

[1]Perusahaan Listrik Negara, Jakarta 12160
[2] Chemical Engineering Program, Institut Teknologi Bandung, Bandung, 40132
Email: veri.hendrayawan@pln.co.id

Abstract. This study evaluates the optimization of Carbon Capture and Storage (CCS) implementation in a subcritical Coal Fired Power Plant (CFPP). The objective of this paper is to investigate how heat integration can reduce energy consumption of CCS systems and analyze their impact on the overall energy penalty of CFPP. The research focuses on a CFPP with an installed capacity of 3×330 MW and design efficiency of 38.4%. The results of the baseline case without heat integration indicate that achieving a 90% CO_2 capture rate using an MDEA+PZ solvent requires a reboiler energy consumption of 3.46 MJ/kgCO_2, which results in an energy penalty of 34% relative to the total energy generated by the CFPP and reduces the overall plant efficiency to 27.4%. Process optimization was identified through the utilization of waste heat. Among all the scenarios evaluated, Case 6, which integrates a rich solvent preheater and an inter-stage heater, achieves the highest energy savings, with up to a 40% reduction in reboiler energy consumption to 2.07 MJ/kgCO_2 and a 10.7% decrease in the overall energy penalty of the CFPP. These findings highlight that strategic heat integration mitigates the energy impacts of CCS implementation which could reduce energy penalty of CFPP.

Keywords: *Optimization, Carbon Capture and Storage, Coal Fired Power Plant, Heat Integration*

1 Introduction

The urgency to address climate change has accelerated global efforts toward achieving Net Zero Emissions (NZE) by the mid-21st century[1]. In this context, decarbonizing the power generation sector which remains a major contributor to CO_2 emissions has become critically important [2]. Despite the steady increase in renewable energy deployment, fossil-fueled power plants are projected to continue playing a critical role in the global energy mix in the foreseeable future, highlighting the urgent need for effective carbon capture and storage (CCS) technologies [3]. Among various CO_2 mitigation strategies, post-combustion CO_2 capture via absorption processes has emerged as the most mature and extensively researched approach for large-scale applications, especially in the context of retrofitting existing power generation facilities[4]. Amine-based solvent systems have been extensively utilized in post-combustion

CO_2 capture (PCC) processes owing to their high reactivity and ease of operation [5]. Nevertheless, these systems incur a substantial energy penalty, primarily stemming from the solvent regeneration step in the stripper, which contributes to over 30% of the power plant's total energy consumption [6]. Consequently, the integration of PCC may cause an overall efficiency to decline of up to 20%, posing a considerable challenge to their economic feasibility. In the case of Indonesia, retrofitting coal-fired power plants with CCS is projected to elevate the Levelized Cost of Electricity (LCoE) by approximately two to three times relative to the current LCoE [7].

To address these challenges, research efforts have increasingly focused on enhancing the performance of PCC through process flow sheet modifications and the development of advanced solvent technologies with lower regeneration energy requirements[3]. The reviewed article consolidates research on process modification strategies for CO_2 capture, which are classified into three main categories: absorption enhancement, focusing on improved CO_2 absorption efficiency[8], heat integration, aimed at maximizing the utilization of thermal energy within the system[9][10]; and heat pump processes, which employ mechanical work such as compression to enhance solvent regeneration efficiency [11][8]. A reboiler energy reduction of up to 45% has been reported by combining parallel economizers with rich solvent splitters, rich solvent preheating, multi-effect strippers, and split flow configurations. In a similar effort, [4] provides a comprehensive review of process modification strategies, classifying them into three primary categories: absorption enhancement, stripping enhancement, and multi-enhancement configurations. The study concludes that the integration of lean vapor recompression, absorber intercooling, and cold solvent bypass yields the greatest reduction in reboiler energy demand up to 50% savings.

The integration of coal-fired power plants (CFPP) with CCS systems presents a distinct profile of waste heat sources compared to other industries, such as oil and gas, thereby requiring further investigation into integration processes. Specifically, six heat integration schemes are evaluated, namely the base case, rich solvent preheater, rich solvent preheater design 2, split flow arrangement, stripper interstage heater, and the combination of rich solvent preheater and interstage heater, as well as comparing their effects on reboiler energy and CFPP energy penalty.

2 Methodology

Process simulation was conducted using Aspen HYSYS V14 to model a subcritical coal-fired power plant (CFPP) and post-combustion CO_2 capture (PCC). The power plant model was based on mass and energy balance data

from an Indonesian CFPP, while the flue gas parameters are used as input for the CCS simulation model. The CCS system design included CO_2 capture and compression unit. Waste heat sources were identified from the baseline CCS-CFPP integration, followed by hot and cold stream mapping and thermodynamic analysis. Heat integration modeling was performed in Aspen Energy Analyzer to generate composite curves and evaluate integration scheme [12].

2.1 Power Plant Model

The power plant modeled in this study is a subcritical coal-fired power plant (CFPP) with a capacity of 3×330 MW and a thermal efficiency of 38.4%. The existing CFPP utilizes a subcritical boiler fueled by lignite coal, with a boiler efficiency of 92.7% [13]. The main steam is generated at a pressure of 174.3 bar and a temperature of 539°C, supplying steam to the high-pressure (HP), IP, and LP turbines. In this case, the flue gas is processed in a shared CCS facility. The plant has a baseline CO_2 emission intensity of 1.02 tCO_2/MWh, with the flue gas composition [14] summarized in Table 1. The modeling of this CFPP assumes identical mass and energy balance parameters across all three CFPP units.

Table 1 Flue Gas Temperature Profile

Parameter	**Concentration**
CO_2	13.8%
O_2	2.16%
N_2	70.08%
H_2O	13.3%
SO_x	844 ppm
NO_x	164 ppm

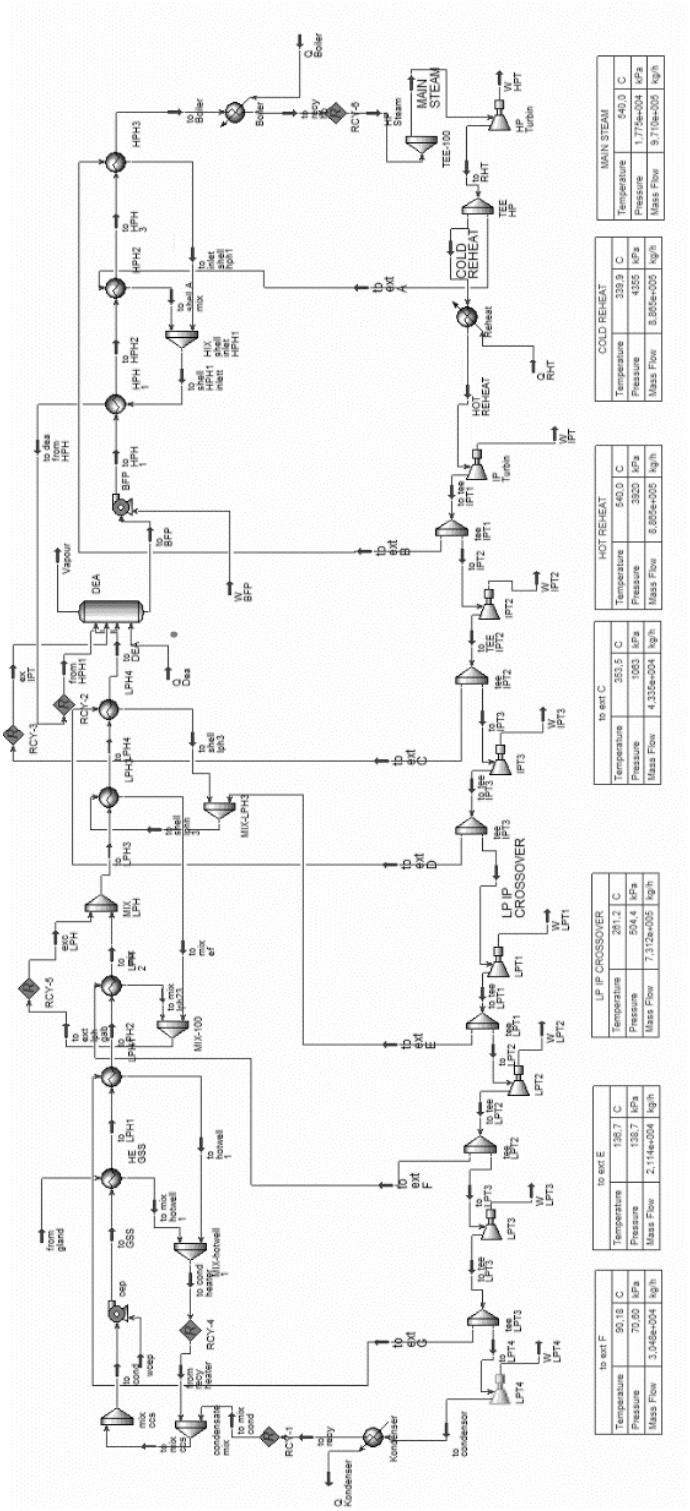

Figure 1 CFPP 330 MW Model

The CFPP was modeled in Aspen HYSYS (Figure 1) and validated against design mass and energy balance for gross power and power plant efficiency. The model assesses the impact of reduced steam flow to the CCS reboiler and its effect on lowering the overall energy output of the CFPP.

The selection of tapping points can be made based on the available steam sources within the plant. The mass and energy balance of the power plant, shown in Figure 1, was used to identify and select potential steam tapping points from the existing plant. A technical comparison was then conducted to evaluate the required steam mass flow to the reboiler and the resulting energy penalty. The identified tapping point options from the baseline plant model are presented in Table 2.

Table 2 Steam Tapping Option

Tapping	Pressure (bar)	Temperature (°C)	Enthalpy (kJ/kg).	Mass Flow (ton/h)
LP/IP Crossover	5.04	261	2983	731
Cold Reheat	43.5	339	3056	880
Main Steam	177	540	3392	969

2.2 Carbon Capture Model

The CO_2 capture process was modeled based on the flue gas parameters, targeting a 90% capture rate using the Shell-Cansolv solvent (MDEA+PZ) and Fluid Package used in the simulation is Acid Gas-Chemical Solvent [15]. The CCS design was developed with reference to prior studies to ensure alignment with established process configurations [16]. The flue gas from each CFPP unit undergoes treatment in a flue gas desulfurization (FGD) system to reduce SO_x content. Subsequently, the flue gas pressure is adjusted by increasing it to 1.2 bar, while the temperature is conditioned at 40°C prior to entering the absorber column. This pressurization is implemented to enhance the CO_2 partial pressure, which facilitates the optimization of CO_2 separation efficiency in the absorber [17]. The CCS process model developed in Aspen HYSYS is illustrated in Figure 2.

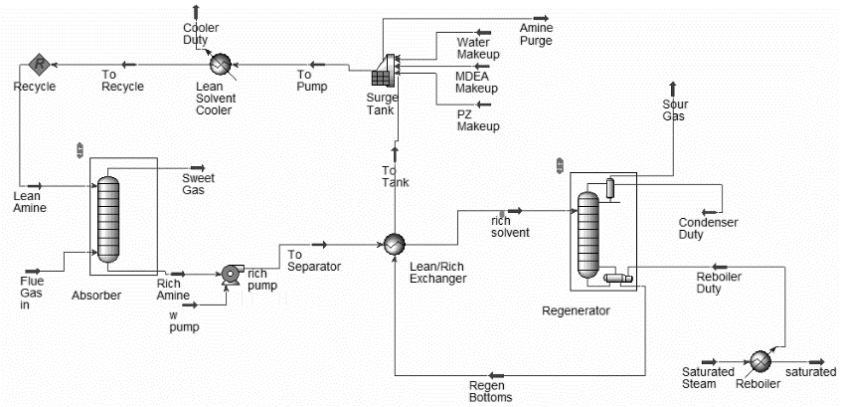

Figure 2 Carbon Capture Modelling

The CCS model aims to determine the reboiler duty and the steam consumption required from the power plant. The CO_2 compression process is designed with four compression stages, achieving a final pressure of 110 bar in the supercritical phase [18] for subsequent storage in an aquifer assumed located 50 km from the existing power plant. The CO_2 compression process model is illustrated in Figure 3. The design parameters employed in the simulation are summarized in Table 3.

Table 3 CCS Design Parameter

Unit	**Parameter**	
Absorber	Type	: Bubble Cap Tray
	Number of Stages	: 40 stages
	Diameter	: 22 m
	Absorber Pressure	: 1.2 bar
	Flue Gas Temperature	: 40 °C
Regenerator	Type	: Bubble Cap Tray
	Number of Stages	: 20 stages
	Diameter	: 15.8 m
	Regenerator Pressure	: 1.8 bar
	Temperature	: 120 °C
Heat Exchanger	ΔTmin	: 10 °C
Loading	Rich Loading	: 0.48 CO_2/Amine
Duty	Regenerator Duty	: 2,9e^9 kJ/h
Compressor	CO_2 Outlet Pressure	: 110 bar
	Compression Stage	: 4 stages

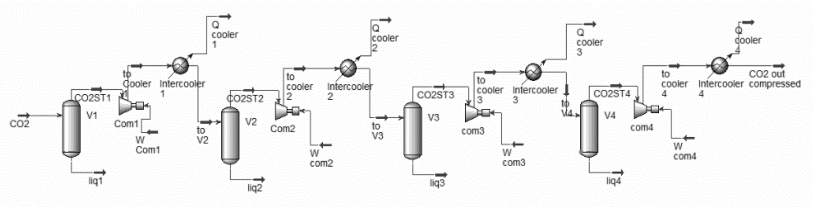

Figure 3 CO_2 Compression Modelling

2.3 Heat Integration Modelling

This study employs a modelling approach to simulate heat transfer within the heat exchanger. The heat balance is determined by quantifying the heat released by the hot fluid and the heat absorbed by the cold fluid. It is assumed that no heat is lost to the surroundings, ensuring that the heat released equals the heat absorbed.

$$Q=U.A.F.\Delta T_{lm} \tag{1}$$

The heat transfer rate is subsequently calculated based on the inlet and outlet temperatures of each fluid, the mass flow rate, and the specific heat capacity of the fluids [19]. The logarithmic mean temperature difference (LMTD) method is used to calculate the average temperature difference between the hot and cold fluids. This value is then utilized to assess the performance of the heat exchanger, taking into account the heat transfer surface area and the heat transfer efficiency

$$\Delta T_{lm} = \frac{(T_{hi} - T_{co}) - (T_{ho} - T_{ci})}{ln \frac{(T_{hi} - T_{co})}{(T_{ho} - T_{ci})}} \tag{2}$$

In the heat exchanger network concept, the pinch method is applied where the heat transfer calculation in pinch analysis is performed using the enthalpy difference, which is obtained by multiplying the heat capacity flow rate (Cp) by the temperature difference between the target temperature and the initial temperature [20]. This method is used to determine the heating and cooling requirements and to identify the pinch point, which represents the minimum temperature difference separating the heating and cooling demands within the system. This approach facilitates the design of an energy efficient heat integration system.

$$\mathrm{Q} = \int_{Ts}^{Tt} Cp.dT = \Delta H \tag{3}$$

The process modelling results of the CFPP and CCS were used to identify the potential for waste heat utilization, as presented in Table 4. In this study, the heat integration model includes two main streams requiring heat input to optimize the CCS process. The application of rich solvent preheating and an interstage heater aims to reduce the reboiler energy demand by lowering the sensible heat, as expressed by the following equation[21].

$$Q_{reg} = (m_{solvent} + m_{CO2})\, Cp\, (T_{reg} - T_{st,in}) + \Delta H_{abs}\, n_{CO2} + \Delta H_{vap,\,H20} \frac{PH20}{PCO2}\, n_{CO2} \quad (4)$$

Table 4 Stream Energy Identification

		Inlet		Outlet		ΔT	Q
Hot Stram	**ton/h**	**bar**	**°C**	**bar**	**°C**	**°C**	**kW**
Intercooling 1	841	5.4	148.6	5.4	40	108.6	3.0×10^4
Intercooling 2	827	16.2	148.9	16.2	40	108.9	2.4×10^4
Intercooling 3	823	50.6	143.2	50.6	40	103.2	2.8×10^4
Intercooling 4	822	110	115.7	110	40	75.7	4.6×10^4
Flue gas	4061	1	141.8	1	40	101.8	2.5×10^5
Overhead Stripper	842	1.8	105	1.8	48	57	3.6×10^5
Cold stream	**ton/h**	**bar**	**°C**	**bar**	**°C**	**°C**	**kW**
Solvent Preheater	9147	2	95	2	110	15	4.7×10^5
Interstage Heater	1444	1.8	118.8	1.8	119.5	0.7	1.7×10^5

The thermodynamic parameters of each stream were mapped to identify heat recovery opportunities within the system. A cascade diagram and a composite curve were then developed using a minimum temperature difference (ΔT_{min}) of 10°C. This approach was selected to balance technical optimization with financial feasibility[12]. The heat integration scheme was developed using Aspen Energy Analyzer, with the heat exchanger network (HEN) design summarized and illustrated in Figure 4. In this study, six process cases were evaluated to improve the energy efficiency of the CO_2 capture system. Case 2 modified the Rich Solvent Preheater (RSP) to raise the rich solvent temperature entering the regenerator, reducing sensible heat demand. Case 3 applied a split-flow RSP design downstream of the rich pump to maximize heat recovery and achieve a higher temperature rise. Case 4 investigated the effect of parallel rich solvent injection at stages 1 and 10 on sensible heat reduction. In Case 5, an additional heater at stages 18–19 enhanced the CO_2 separation driving force, increasing stripper temperature, and lowering reboiler duty. Finally, Case 6 combined the interstage stripper modification with the RSP to assess potential synergistic benefits. The heat exchanger modeling assumes that ambient temperature does not affect the heat transfer effectiveness.

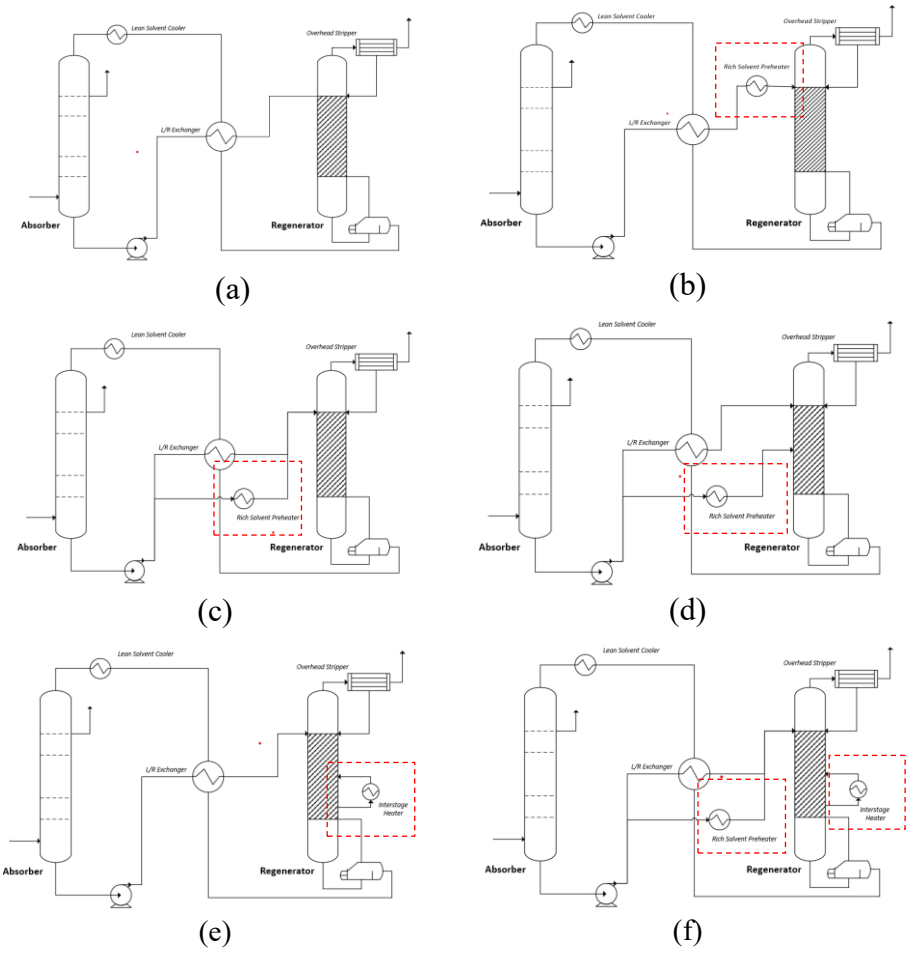

Figure 4. Case Heat Integration. (a) Case 1 Base Case (b) Case 2 Rich Solvent Preheater (c) Case 3 Rich Solvent Preheater Design 2 (d) Case 4 Split Flow Arrangement (e) Case 5 Stripper Interstage Heater (f) Case 6 Rich Solvent Preheater and Interstage Heater Combination

3 Result and Discussion

3.1 Base Case Model

In the base case modeling, capturing 90% of CO_2 from the 3×330 MW subcritical power plant requires a reboiler duty of 3.46 GJ/tCO_2. The model was validated using reboiler duty data from previous studies[22][23]. A comparative analysis of the tapping point options was carried out to assess steam mass flow requirements, energy penalties, unit efficiency impacts, and potential

operational challenges. The LP/IP crossover delivered the highest gross output of 270.2 MW with a steam requirement of 414.3 ton/h, achieving the lowest energy penalty 33.7% and highest efficiency 27.4%. In comparison, cold reheat produced 210.6 MW at 399.0 ton/h of steam with a 52.0% energy penalty. while main steam tapping, although requiring the least steam 355.7 ton/h, yielded the lowest output 191.3 MW and highest energy penalty 57.9%. Overall, the LP/IP crossover configuration provides clear operational and energetic advantages, reducing the energy penalty by up to 24 percentage points and improving gross output by nearly 79 MW compared to main steam tapping. Beyond technical factors, operational considerations must also be addressed. For example, the cold reheat tapping point may risk overheating the boiler's reheater tubes, the IP extraction point could affect deaerator operation, and the existing LP extraction point may not supply sufficient steam mass flow to meet the CCS system's requirements.

Table 5 Steam Tapping Evaluation

Tapping	Steam Req (ton/h)	Gross Out (MW)	Energy Penalty (%)	Efficiency (%)
Main Steam	355.7	191.3	57.9	18.5
Cold Reheat	399.0	210.6	52.0	21.4
LPIP Crossover	414.3	270.2	33.7	27.4

3.2 Heat Integration Model

The heat integration scheme identifies the potential recoverable heat, as summarized in Table 4. Using this stream data, a composite curve was developed to determine the pinch temperature, which served as the basis for designing the heat exchanger network integration.

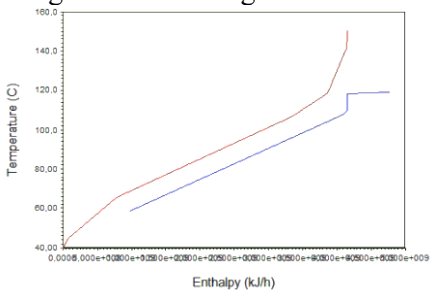

Figure 5 Composite Curve Case 6

Case 2. The rich solvent preheater raises the temperature of the rich solvent before it enters the regenerator. In the baseline simulation, the

solvent reached ~94°C, constrained by the lean-rich heat exchanger's minimum temperature difference (ΔT_{min}) of 10°C to ensure retrofit feasibility. Incorporating a parallel economizer increased the rich solvent temperature to 97.9°C, reducing reboiler duty by 15.3% to 2.93 GJ/tCO_2.

Case 3. In Case 2, the system was further optimized by introducing a 3:1 split flow of the rich solvent at the rich pump outlet, effectively dividing the duty of the lean-rich heat exchanger. This configuration was enhanced by a parallel economizer that utilized waste heat sources identified in Table 4. As a result, the outlet temperature of the lean-rich heat exchanger increased from 94°C in the baseline case to 106°C, achieving a 30% reduction in reboiler duty and lowering the energy penalty to 28.4%.

Case 4. In the split-flow configuration, the rich solvent stream was divided at an 8:1 ratio to enter the regenerator at stage 1 and stage 10, respectively. The lean-rich heat exchanger raised the solvent temperature to 102°C before entry at stage 1, while a parallel heat exchanger further increased the temperature to 177.2°C for injection at stage 10. This configuration resulted in a 29% reduction in reboiler duty and lowered the energy penalty to 30% of the power plant's capacity.

Case 5. An interstage heater was installed between stages 18 and 19 of the regenerators. At stage 19, the solvent temperature increased from 118.8°C to 119.2°C using a solvent mass flow ratio of 1:6 relative to the total regenerator flow. This adjustment reduced the reboiler thermal duty to 2.94 GJ/tCO_2. However, the additional heating represented a significant energy input, effectively substituting part of the reboiler demand and redistributing heat duty across the column. Overall, the configuration achieved a 15% reduction in reboiler duty and lowered the power plant's energy penalty to 31.7%.

Case 6. A combination of the interstage heater and rich solvent preheater was applied by utilizing the remaining heat from Case 5 to further preheat the rich solvent. In this configuration, the solvent temperature at stage 18 increased from 118.8°C to 119.2°C, while the residual heat raised the rich solvent temperature from 59°C to 104.6°C. Integrating these approaches resulted in a 40% reduction in reboiler duty and lowered the energy penalty to 26%.

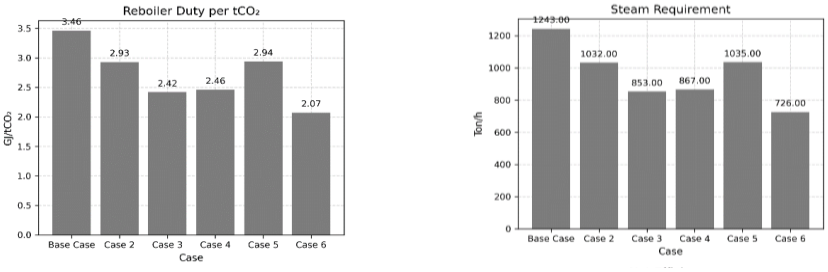

(a) (b)

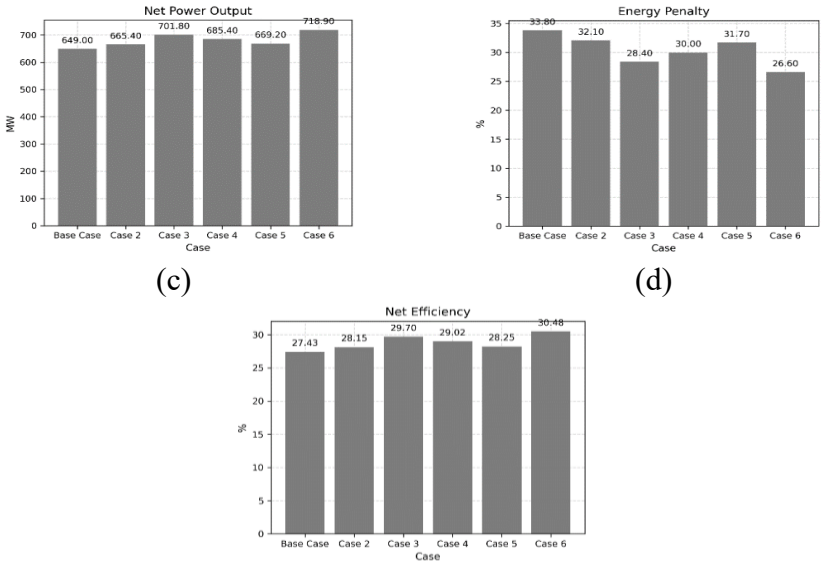

Figure 6 Comparation Result (a) Reboiler Energy (b) Steam Requirement (c) Net Power Output (d) Energy Penalty (e) Net Efficiency

The observed temperature profiles highlight the distinct effects of interstage heating and rich solvent preheating on regenerator performance. The interstage heater improved the temperature at stage 18, lowering the reboiler duty by enhancing the CO_2 release driving force. Meanwhile, the rich solvent preheater increased the inlet temperature of the rich solvent, leading to a decrease in sensible heat demand due to a reduced temperature gap relative to the reboiler. The temperature profile for each stage is presented in Figure 8.

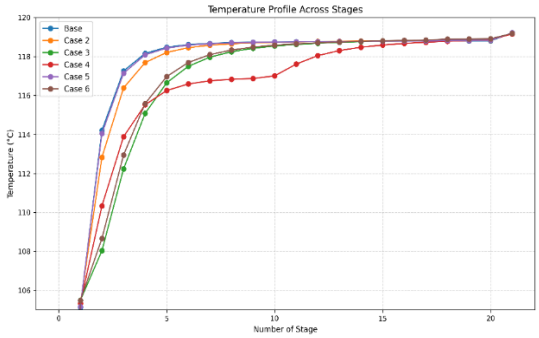

Figure 7 Temperature Profile Across Stages

Future research should further investigate the cost of process modifications, perform detailed economic sensitivity analyses, and evaluate the potential broader impacts on the power grid system.

4 Conclusion

Retrofitting a 3×330 MW subcritical coal-fired power plant with CCS requires a reboiler energy of 2.9×10^9 kJ/h, resulting in an energy penalty of 34% and a reduction in plant efficiency to 29.7%. When evaluating steam tapping locations, the LP-IP crossover point was found to deliver the lowest energy penalty at 24%, compared to main steam or cold reheat tapping points. Additionally, the LP-IP crossover posed fewer operational risks than the other tapping options. To mitigate the CCS energy penalty, this study explored heat integration strategies by utilizing waste heat identified from the integrated CFPP-CCS system. Several heat integration scenarios were modeled and compared using Aspen Energy Analyzer to assess their effects on the CCS reboiler duty. Reducing the reboiler duty translates directly into lower steam demand from the power plant, thereby reducing the overall energy penalty. Among the evaluated scenarios, Case 6 combining rich solvent preheating with an interstage regenerator heater achieved the highest improvement, reducing the reboiler duty by 40% to 2.07 GJ/tCO_2. This reduction lowered the energy penalty to 26% and increased net power output by 10.6%.

References

[1] S. Report, “Climate Change 2023 Synthesis Report,” 2023.

[2] Y. M. Chen, H. J. Hsu, and Y. J. Lin, “Improving CO_2 Capture Efficiency with High-Capacity Solvents: Addressing Temperature-Induced Mass Transfer Limitations,” *Ind. Eng. Chem. Res.*, vol. 64, no. 4, pp. 2283–2293, 2025, doi: 10.1021/acs.iecr.4c03453.

[3] Y. Le Moullec and T. Neveux, *Process modifications for CO_2 capture*. 2016. doi: 10.1016/B978-0-08-100514-9.00013-5.

[4] O. Khalifa, I. I. I. Alkhatib, D. Bahamon, A. Alhajaj, M. R. M. Abu-Zahra, and L. F. Vega, “Modifying absorption process configurations to improve their performance for Post-Combustion CO_2 capture – What have we learned and what is still Missing?,” *Chem. Eng. J.*, vol. 430, no. October 2021, 2022, doi: 10.1016/j.cej.2021.133096.

[5] IEAGHG, “Techno Economic Evaluation of Different Post Combustion CO_2 Capture Process Flow Sheet”, 2014/08, August 2014.

[6] M. I. Taipabu, K. Viswanathan, W. Wu, R. Handogo, A. Mualim, and H. Huda, “New improvement of amine-based CO_2 capture processes using heat integration and optimization,” *Chem. Eng. Process. - Process Intensif.*, vol. 193, no. August, p. 109532, 2023, doi:

10.1016/j.cep.2023.109532.
[7] S. Adisasmito, A. Raksajati, A. Ali, H. Susilo, M. A. Susetyo, and A. M. Reza, "Modelling of Carbon Capture Process for Coal-Fired Power Plants in Indonesia," *cetjournal.it*, vol. 106, pp. 961–966, 2023, doi: 10.3303/CET23106161.
[8] H. Ahn, M. Luberti, Z. Liu, and S. Brandani, "Process configuration studies of the amine capture process for coal-fired power plants," *Int. J. Greenh. Gas Control*, vol. 16, pp. 29–40, 2013, doi: 10.1016/j.ijggc.2013.03.002.
[9] P. P. Data, P. Examiner, M. C. Mayes, F. Application, and P. Data, "(12) United States Patent," vol. 2, no. 12, 2011.
[10] M. I. Taipabu, K. Viswanathan, W. Wu, R. Handogo, A. Mualim, and H. Huda, "New improvement of amine-based CO_2 capture processes using heat integration and optimization," *Chem. Eng. Process. - Process Intensif.*, vol. 193, no. June, p. 109532, 2023, doi: 10.1016/j.cep.2023.109532.
[11] E. Sanchez, E. J. Bergsma, F. De Miguel, E. L. V Goetheer, and T. J. H. Vlugt, "International Journal of Greenhouse Gas Control Optimisation of lean vapour compression (LVC) as an option for post-combustion CO 2 capture : Net present value maximisation," *Int. J. Greenh. Gas Control*, vol. 11, pp. 114–121, 2012, doi: 10.1016/j.ijggc.2012.09.007.
[12] B. Linnhoff and S. Ahmad, "Cost optimum heat exchanger networks-1. Minimum energy and capital using simple models for capital cost," *Comput. Chem. Eng.*, vol. 14, no. 7, pp. 729–750, 1990, doi: 10.1016/0098-1354(90)87083-2.
[13] PLN, "Performance Test Report Unit3 Vol I", 2011.
[14] PLN, "Performance Test Report Unit3 Vol 2", 2011.
[15] S. Mudhasakul, H. Ku, and P. L. Douglas, "International Journal of Greenhouse Gas Control A simulation model of a CO 2 absorption process with methyldiethanolamine solvent and piperazine as an activator," vol. 15, pp. 134–141, 2013.
[16] J. Gervasi, L. Dubois, and D. Thomas, "Simulation of the post-combustion CO_2 capture with Aspen HysysTM software: Study of different configurations of an absorptionregeneration process for the application to cement flue gases," *Energy Procedia*, vol. 63. pp. 1018–1028, 2014. doi: 10.1016/j.egypro.2014.11.109.
[17] M. M. F. Hasan, E. L. First, F. Boukouvala, and C. A. Floudas, "A multi-scale framework for CO_2 capture, utilization, and sequestration: CCUS and CCU," *Comput. Chem. Eng.*, vol. 81, pp. 2–21, 2015, doi: 10.1016/j.compchemeng.2015.04.034.
[18] S. Yang *et al.*, "Process Design and Cost Estimation of Carbon Dioxide Compression and Liquefaction for Transportation," *Korean Chem. Eng. Res.*, vol. 50, no. 6, pp. 988–993, 2012, doi: 10.9713/kcer.2012.50.6.988.

[19] D. E. Yabrudy-Mercado, B. S. S. López-Sarria, J. G. Fajardo-Cuadro, and C. A. Cardona-Agudelo, "Indicators for maintenance planning based on energy efficiency in heat exchanger networks," *Sci. Tech.*, vol. 25, no. 3, pp. 367–371, 2020, doi: 10.22517/23447214.23621.

[20] I. C. Kemp, "Introduction," *Pinch Anal. Process Integr.*, pp. 1–13, Jan. 2007, doi: 10.1016/B978-075068260-2.50006-7.

[21] A. Raksajati, M. T. Ho, and D. E. Wiley, "Understanding the Impact of Process Design on the Cost of CO_2 Capture for Precipitating Solvent Absorption," *Ind. Eng. Chem. Res.*, vol. 55, no. 7, pp. 1980–1994, 2016, doi: 10.1021/acs.iecr.5b03633.

[22] B. Zhao *et al.*, "Enhancing the energetic efficiency of MDEA/PZ-based CO_2 capture technology for a 650 MW power plant: Process improvement," *Appl. Energy*, vol. 185, pp. 362–375, 2017, doi: 10.1016/j.apenergy.2016.11.009.

[23] X. Wang, F. Zhang, L. Li, H. Zhang, and S. Deng, *Carbon dioxide capture*, vol. 58. 2021. doi: 10.1016/bs.ache.2021.10.005.